Ionization and Fragmentation of 5-Chlorouracil induced by 100 keV protons collisions

Pierre Cafarelli[a], Pierre Çarçabal[a,b], Jean-Philippe Champeaux[a], Arnaud Le Padellec[a], Patrick Moretto-Capelle[a], Julien Rabier[a], Martine Sence[a]

[a]*Laboratoire Collisions, Agrégats, Réactivité, UMR 5589, CNRS-Université Paul Sabatier Toulouse 3, IRSAMC, 31062 Toulouse Cedex 9, France*
[b]*Laboratoire de Photophysique Moléculaire CNRS, UPR 3361, Batiment 210, Université Paris Sud, 91405 Orsay cedex, France*

Abstract. We present preliminary experimental results on the dissociation of singly and doubly ionized 5-Chlorouracil induced by collisions with proton of 100 keV energy. Multiple coincidence techniques are used to detect the ionic fragments from single dissociation events. This enables a thorough analysis of kinetic momentums of the charged and neutral species involved in the dissociation. In many cases, this leads to the establishment of the scenario the molecule undergoes after ionization as well as the determination of the nature of intermediate (undetected) species. In other cases, the dissociation scenario cannot be unambiguously identified and further analysis as well as theoretical support is needed.

Keywords: Halogenated uracil, radiosensitizer, proton collision, multiple coincidence detection.
PACS: 34.50.Gb

INTRODUCTION

Proton therapy is a powerful non-ablasive, conformational radiotherapy with the advantage of delivering a precise dose at a given depth, owing to the localization of the Bragg peak [1,2,3]. It indicates that incident protons have a maximum energy deposition in and efficient interaction with irradiated tissues when they have lost enough of their initial energy to reach about 100 keV. The depth of the Bragg peak is adjustable by varying the energy of the incident proton beam (typically of the order of several MeV), only little energy being dissipated in the tissues before and nearly none after. Consequently, in spite of the technological difficulties it implies, this technique is used as widely as possible in combination with chemotherapies and with the use of radio-sensitizing molecules [4]. Halogenated uracils are often found in such treatments either in the chemotherapy step or as radio-sensitizers themselves. Unfortunately, little is known about what makes, *a priori*, a given molecule a good radiosensitizer.

In order to better understand the primary processes involved in radiosensitizing at the molecular level, we have undertaken a systematic study of the damages (ionization and fragmentation) occurring after collisions of protons of 100 keV energy (in order to mimic the condition imposed by the Bragg peak) on halogenated uracil species. These studies are completed in the gas phase in view of addressing the intrinsic properties of the molecules under investigation, with the aim of providing benchmark information to test, validate and hopefully feed more global views and models on radiation damage and radiotherapy.

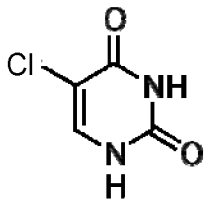

FIGURE 1. Chemical structure of 5-ChloroUracil (5ClU); mass=146 amu.

CP1080, *Radiation Damage in Biomolecular Systems, Proceedings of the 5th International Conference (RADAM)*
edited by Károly Tőkési and Béla Sulik © 2008 American Institute of Physics 978-0-7354-0611-7/08/$23.00

After describing our experimental approach, we report here preliminary results obtained on 5-ChloroUracil (5ClU, mass 146 amu, see figure 1). Fragmentation products emerging from both singly and doubly ionized 5ClU have been observed. In the case of double ionization, the analysis method, taking full advantage of the multiple correlation detection used here can lead to the decomposition of the fragmentation process in consecutive sequential steps. Two dissociation channel cases are reported: in the first one, conclusive identification of a 3-body sequential dissociation channel is given by the direct analysis of the experimental results, while the analysis of the second case leads to less unambiguous conclusions and further analysis, complemented by theoretical chemistry back up will be needed to establish how the observed product ions are formed.

EXPERIMENTAL SETUP

The projectile ion beam is obtained from a RF discharge of molecular hydrogen which produces a mixture of H^+, H_2^+ and H_3^+ ions, extracted by a potential of about 1keV. The emerging ion beam is focused before being accelerated by a 1 meter long accelerator made of 24 electrodes, generating a self-focusing electrostatic field. The ions then reach a steering electro-magnet where the mass to charge ratio of the desired projectiles is selected and they are sent towards the collision chamber through the ion optics line at an angle of 60° with respect to the accelerator. In this line, the ion beam crosses a set of lens and deviators and is ultimately collimated through two 2 mm holes separated by about 50 cm, the last one being located 4 cm before the collision region. Before the collimating holes, the continuous ion beam is deflected to impinge onto a pulser plate and the deflection is periodically turned off to let the ions cross a slit in this plate. This results in the production of a pulsed ion beam with tunable repetition rate and duty cycle. In the experiments reported below, we have used 100 keV protons as projectiles. Once they have reached the collision chamber, the projectiles interact with the target molecule in the extraction region of a linear Time-Of-Flight (TOF) mass spectrometer (MS) of 175 mm in length.

The target molecules are sublimated at a temperature of about 400 K in an oven located in the collision chamber. In a matrix isolation spectroscopy study [5], Kolos *et al.* have observed the infrared vibrational spectrum of 5ClU trapped in solid argon after sublimation in conditions similar to ours and there is no evidence in the spectra for the presence of a significant amount of thermal decomposition and all the observed bands could be assigned to 5ClU. In order to maximize the target density in the collision volume, the outlet of the oven is placed as close as possible to the repeller plate of the TOF MS where a 2 mm hole lets the effective part of effusive beam reach the extraction region. In order to minimize contamination of the MS by target molecules that would condense on the electrodes, the oven makes a 30° angle with the TOF axis. Hence, most of the target beam condenses on the back of the repeller and extractor plates, leaving the rest of the MS clean. The powder of 5ClU was purchased from Sigma-Aldrich and used without any further purification. However, the oven was outgased at least one day before measurements by being slowly heated. This substantially reduced, but not removed completely, the amount of water in the collision region. The ion optics line and collision chamber were kept at a pressure in the low 10^{-7} Torr while measurements were performed.

After the neutral target – ionic projectile collisions have taken place, the product ions are mass to charge analyzed by the TOF MS operating in second order focusing [6]. A delayed pulsed extraction field of 500V/cm with a 10 ns rise time is triggered once the bunch of projectile ions has crossed the collision region so that the TOF of ions produced at the beginning and at the end of a given projectile ions bunch is essentially identical. This substantially improves the time and, therefore, mass resolution of the MS. Between two pulses a small continuous field of about 5V/cm is kept in the extraction region in order to evacuate any residual ions. After being post-accelerated, the ions are counted on a multi-channel plate (MCP) detector, in front of which a negatively biased grid repels the secondary electrons, so that the detection efficiency is greatly enhanced from 60% up to 95% [7], the collection efficiency of the TOF MS is about 85% owing to the high extraction field with respect to the limited kinetic energy imparted to the fragments of the order of few eV [8]. The whole setup polarity can be inverted in order to detect either positively charge or negatively charged ions.

The repetition rate of the pulsed proton beam is 20 kHz with a pulse width of the order of few ns. This results in a low intensity incident proton beam interacting with a very low density gas target. Consequently, product ions are detected much less often than once every shot (typically an event is detected every 100 shots). In such a low counting rate regime and with the high detection efficiency of our detector, we can achieve coincidence detection: if two (or more) ions are detected by the MCP within one proton pulse cycle, we can consider that they originate from the fragmentation of the same parent molecule. This is necessary to extract the cinematic information required for the study of the dissociation pathways as will be presented below.

Acquisition is done event by event, an event being characterized by the number of detected fragments and their corresponding time-of-flight. The time of arrival of any charged fragment is registered by means of a fast Comptek 7885 multi-stop module with a 5 ns resolution. Delays control, trigger generation, and mixing of signals are achieved using CO4020 Ortec modules.

RESULTS AND DISCUSSION

Even though both positive and negative product ions have been sought for, only positively charged ions have been detected. Among the detected events, the vast majority (about 90%) was due to single product ions, that is, originating from singly ionized molecules. Another 10% were due to the detection of two product ions corresponding to a doubly charged parent. The events where 3 or more fragments were detected accounted for only a very minute number of cases (less than 1%). This distribution is typical for such measurements and we will focus in what follows on the fragmentation occurring from singly and doubly positively charged 5ClU.

Single Ionization and Fragmentation

The TOF mass spectrum of the product ions arising from single ionization of 5ClU upon collision with 100 keV protons is shown in figure 2.

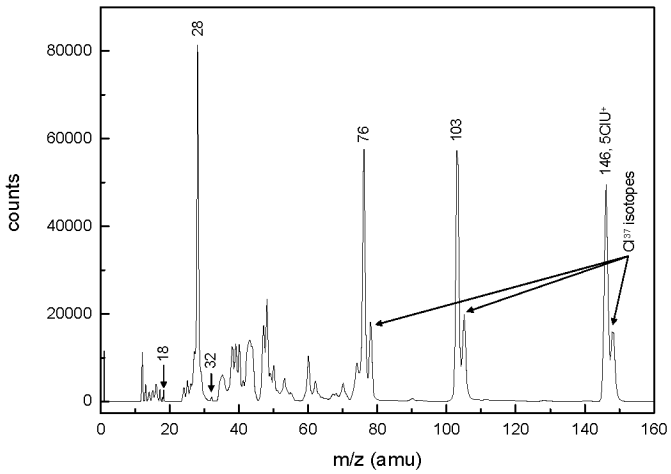

FIGURE 2. TOF mass spectrum of product ions originating from $5ClU^+$.

This spectrum results from the subtraction of the raw data spectrum by a background spectrum recorded without heating the sublimation oven. This removed the contribution from H_2O^+ (m/z=18 amu – an intense peak before subtraction), and OH^+ (17 amu), except for some residual signal due to the substraction. These residual peaks are not disturbing however, since there is no expectation to obtain such masses from fragmenting $5ClU^+$ without substantial post-fragmentation recombination and rearrangements (cf. figure 1), making them quite unlikely. More importantly, upon background subtraction, most of the contribution from O_2^+ (from residual air, mass 32 amu) vanishes and since the ratio $[N_2]/[O_2]$ is around 4 in air, we can conclude that only a small amount (less than 7%) of the dominating mass peak at m/z=28 is due to residual air N_2 and most of it is due to fragmentation of $5ClU^+$ and can be assigned to $HCNH^+$ or CO^+ fragments. Previous studies on similar systems have shown that the production of an $HCNH^+$ fragment should be energetically favored [8].

Chlorine atoms can be found in two stable isotopic forms of mass 35 amu and 37 amu with natural abundances of about 75% and 25%, respectively. Hence the mass peaks of all products ions containing the chlorine atom of $5ClU^+$ must exhibit this typical isotopic separation. In particular, the three last doublets on the high mass end of the spectrum are composed of two well resolved peaks separated by 2 amu with relative intensities of 3:1. This also illustrates the mass resolution achieve on our setup in spite of the relatively small length of the TOF MS. More importantly, this greatly facilitates the attribution of the spectrum since any such doublet must correspond to a fragment containing the chlorine atom. Consequently, the found at m/z=103 can be assigned to a $C_3H_2NOCl^+$ ion

fragment associated to the loss of a neutral OCNH. There are three ways to loose this neutral fragment from 5ClU. This may explain the high intensity of the associated ion mass peak but we cannot favor one particular dissociation channel at this point of the study. There are no obvious way to form the intense mass peak found at m/z=76 without substantial chemistry taking place before or after dissociation and we need further investigation to establish which pathway yields to this fragment.

Double Ionization and Fragmentation

Each event recorded in the correlated two-fragment mass spectrum given in figure 3 corresponds to the detection of two product ions after the interaction between the protons and 5ClU which means they originate from dissociation following the double ionization of 5ClU. The horizontal (resp. vertical) axis of this intensity plot corresponds to the TOF of the lighter (resp. heavier) ion emitted by $5ClU^{++}$. The summed projections on each one of these axis are also shown on the figure together with the mass calibration of the major and most significant peaks.

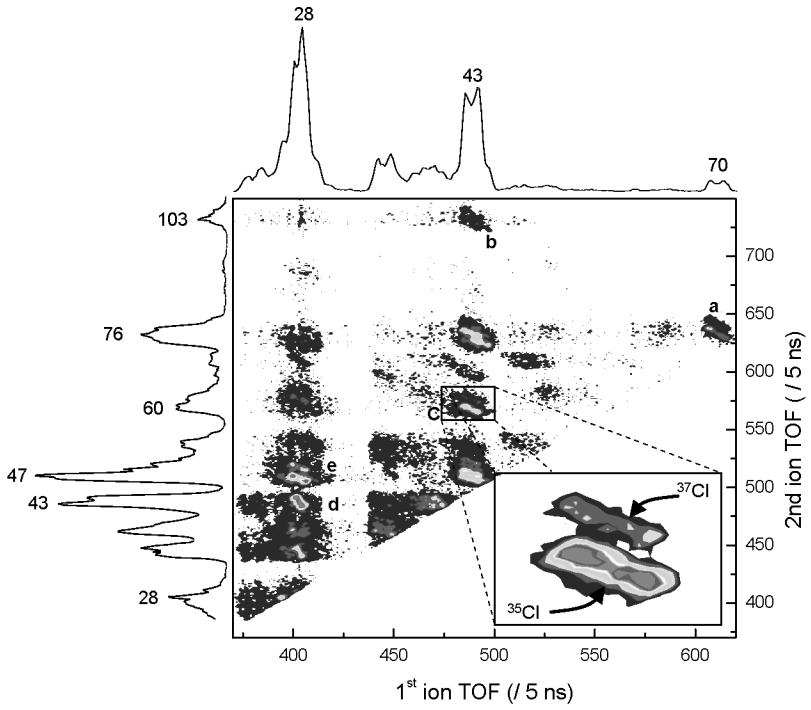

FIGURE 3. Portion of the 2D correlation mass spectrum and projected mass spectra of ion couples produced after double ionization of 5ClU induced by collision with 100 keV protons. The labeled correlation islands are discussed in the text. The inset offers a magnified view of correlation island "c" in order to facilitate the observation of the isotopic doublet.

Because of the time spread due to kinetic energy of the fragments after dissociation (see below for further explanation), there is an apparent loss in resolution on the projection mass spectra compared to the spectrum shown in figure 2. Nevertheless, from inspection of the 2D spectrum, we can observe the separation of the chlorine isotopes (see for example the correlation island "a", "e" in figure 3 and "c" in the inset) which can be used to facilitate the assignment of the observed fragments. For instance, correlation island "e" has a 3 times weaker parallel island just above it, separated by 2amu. The fragment of mass 47 is therefore assigned to CCl^+. Contrarily, the correlation island "d" does not feature the typical isotopic doublet, thus leading to the conclusion that the mass 43 fragment doesn't contain the chlorine atom and is most probably to be assigned to $OCNH^+$ fragments. The peaks at m/z=43 on both projections feature a depletion at their center and appear as unresolved doublets. This profile is not due to two fragments of adjacent mass but to m/z=43 ionic fragments being emitted perpendicularly to the TOF MS axis with large kinetic energy. Such ions escape the MS before being detected which explains the apparent dip in the mass peaks.

Only two correlation islands ("a" and "b" in figure 3) correspond to two body fragmentations pathways where the parent $5ClU^{++}$ ion is split into two ionic moieties. They are minor fragmentation channels as "a", corresponding to $146^{++} \rightarrow 70^{+} + 76^{+}$, and "b" , corresponding to $146^{++} \rightarrow 43^{+} + 106^{+}$, account to less than 3% of the overall counts.

All the other islands correspond to at least 3-body dissociation pathways where two charged fragments and at least one (undetected) neutral fragment are emitted. A given charged particle, emitted with the initial momentum P along the TOF MS axis and within the extraction field E, has its TOF modified compared to its nominal TOF T_0,without initial momentum, according to the relation: $T = T_0 - P/qE$. This time spread is the origin of the observed correlation islands. Hence, in the case of a 3-body dissociation (2 ions i1 and i2, and one neutral n) and assuming the parent $5ClU^{++}$ at rest before dissociation [9], total momentum conservation allows converting the correlation islands TOF(i2) vs. TOF(i1) into 3 correlated momentums plots P(i2) vs. P(i1), P(n) vs. P(i1) and P(n) vs. P(i2). Assuming the recoil energy between fragments being dominated by Coulombic repulsion between ions, simple conservation relations allows using the slopes of these momentums plots to tell which dissociation pathway leads to the observed fragments. Three possible scenarios can lead from an initial ABC^{++} to three fragments A^{+}, B^{+} and C° [10]:

i. Initial charge separation: $ABC^{++} \rightarrow AC^{+} + B^{+} \rightarrow A^{+} + B^{+} + C°$; with $P(B^{+}) = -(m_{AC}/m_{A})\ P(A^{+})$, $P(C°) = (m_{C}/m_{A})\ P(A^{+}) = -(m_{C}/m_{AC})\ P(B^{+})$. This scenario includes two distinguishable pathways with different slopes: one where the first emitted ion is the lighter one and another where it is the heavier.

ii. Deferred charge separation : $ABC^{++} \rightarrow AB^{++} + C° \rightarrow A^{+} + B^{+} + C°$; with a -1 slope between $P(A^{+})$ and $P(B^{+})$ as in a two body dissociation.

iii. Concerted fragmentation: $ABC^{++} \rightarrow A^{+} + B^{+} + C°$; in this instantaneous 3-body fragmentation, the kinetic energy can be randomly distributed over the three fragments and slopes cannot be calculated.

An Identified 3- Body Fragmentation Sequence: The (43^{+},60^{+}) Correlation Island.

The island labeled "c" in figure 3 corresponds to the detection of a light ion of mass 43 and a heavy one of mass 60. Since the island features the chlorine isotopic doublet on the vertical axis but not the horizontal one, the mass 43 ion must be $OCNH^{+}$ and the mass 60 ion can be assigned to $HCCCl^{+}$. If one applies the time to momentum transformation mentioned above, one obtains the correlated momentums plots shown in figure 4.

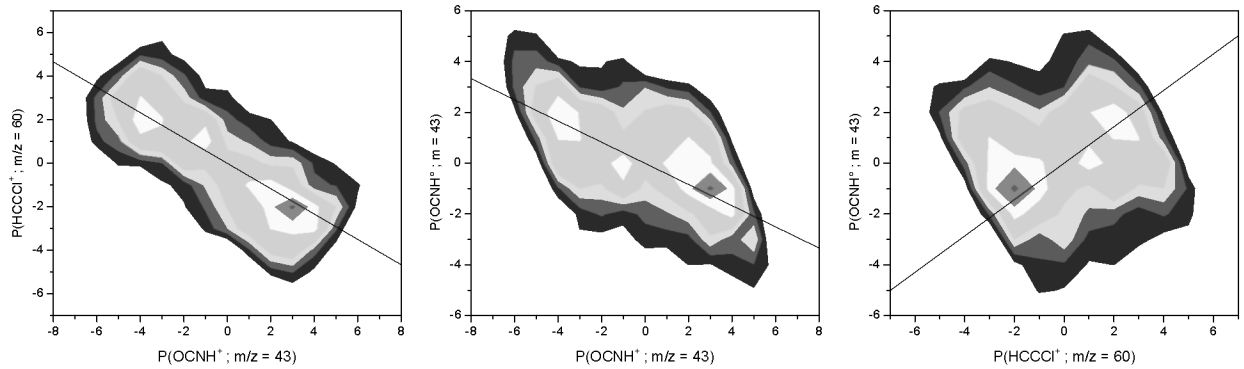

FIGURE 4. Correlated momentums plots (in arbitrary units) obtained from the correlation island "c" of figure 3. Superposed lines have slopes calculated for the dissociation pathway $5ClU^{++} \rightarrow C_3H_2NOCl^{+} + OCNH^{+} \rightarrow HCCCl^{+} + OCNH° + OCNH^{+}$.

A weighted linear least square fit of the plots lead to the set of slopes: $P(60^{+})/P(43^{+})$=-0.59; $P(43°)/P(43^{+})$=-0.41 and $P(43°)/P(60^{+})$=0.65. This excludes a deferred charge scenario (ii) for which a -1 slope is expected for $P(60^{+})/P(43^{+})$. An initial charge separation pathway following the sequence $146^{++} \rightarrow 86^{+} + 60^{+} \rightarrow 43^{+} + 43° + 60^{+}$ can also be discarded as it implies slopes of -2, 1 and -0.5. Finally, the other initial charge separation pathway $146^{++} \rightarrow 103^{+} + 43^{+} \rightarrow 60^{+} + 43° + 43^{+}$ leads to slopes of : -0.58; -0.42 and 0.72. Lines with these expected slopes are superposed to the experimental plots in figure 4. There is a good agreement between expected and experimentally derived slopes and we can conclude with confidence that the dissociation pathway leading to the observation of the correlation island "c" starts with a loss of a $OCNH^{+}$ fragment followed by the dissociation of the remaining moiety into $CHCCl^{+}$ and a unique OCNH° neutral.

The treatment of island "d" of figure 3 leads to the correlated momentums plots shown in figure 5.

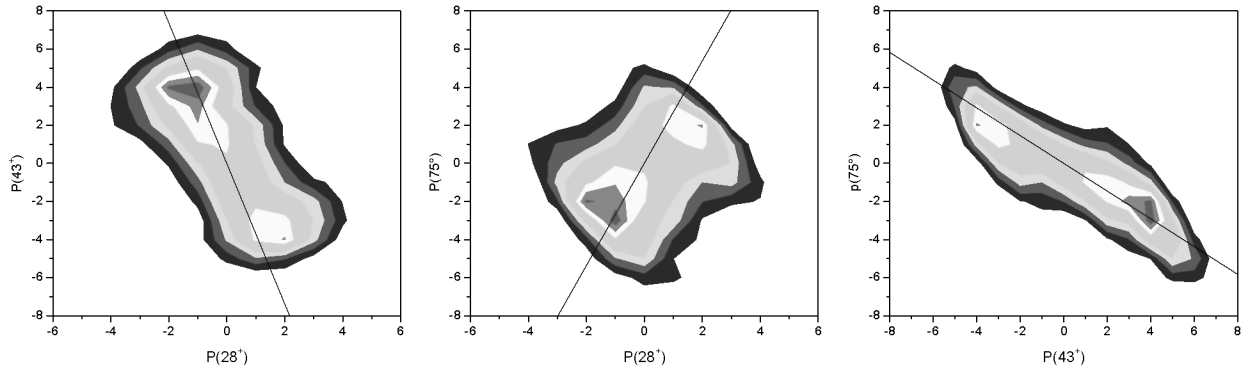

FIGURE 5. Correlated momentums plots (in arbitrary units) obtained from the correlation island "d" of figure 3. Superposed lines have slopes calculated for the dissociation pathway $146^{++} \rightarrow 103^+ + 43^+ \rightarrow 28^+ + 75° + 43^+$.

From this plots, we derive experimental slopes of : $P(43^+)/P(28^+)$=-2; $P(75°)/P(28^+)$=1 and $P(75°)/P(43^+)$= -0.6. The most approaching set of expected slopes is the one associated to an initial charge separation following the sequence: $146^{++} \rightarrow 103^+ + 43^+ \rightarrow 28^+ + 75° + 43^+$. The expected slopes for this scenario are -3.6, 2.7 and -0.7. Lines of such slopes are shown on figure 5. In spite of the obvious numerical discrepancy, we can see that the agreement between experimental and expected slopes is of course not as good as in the previous case but does not let us definitely rule out this scenario. We must then recognize that we cannot conclude with certainty whether $5ClU^{++}$ undergoes this 3-body sequential fragmentation, a 3-body concerted fragmentation (scenario iii) or else a more complex dissociation involving more neutrals to lead to the correlation island "d".

CONCLUSION

We have presented preliminary experimental results on the dissociation after single and double ionization induced by collision between 5-chlorouracil and 100 keV protons.

The analysis of the correlation mass spectra of the product ions originating from $5ClU^{++}$ can, in some case (the (43^+, 60^+) correlation island for instance) lead to the decomposition of the dissociation processes into a sequence. This allows determining the reaction path followed by the system, as well as identifying undetected intermediate species. These are important information that allows modeling such processes along the proper reaction coordinates. In other cases, the identification of the intermediate steps leading to the observed final product ions is not as easy or univocal as it has been shown for the (28^+, 43^+) correlation island.

For the molecule under investigation here, several correlation islands fall into the second situation. Further analysis and the help of theoretical chemistry to attempt simulating the various dissociation pathways and compare their relative probability will be necessary to better understand the radiation induced chemistry taking place. Such studies are now in progress. Also, when 3-body scenarios are among the undecided possibilities, experimental values of the kinetic energy release (KER) can be extracted from the correlated momentums plots. This can help to choose one fragmentation scenario to another when comparing experimental KER values with calculated activation energies associated to all possible scenarios [8]. This illustrates an advantage of studying molecular systems of moderate sizes in the gas phase since it enables conducting quantum chemistry calculation at a fairly high level of theory in order to extract reliable calculated values. Furthermore, we can also detect and perform the spectroscopy of emitted electrons as already achieved in our group for uracil-protons collisions [11]. This is an important measurements as low energy electrons are known to play a crucial role in indirect processes involved in radiation damage [12].

This work is part of a systematic investigation of protons induced damage of halogenated uracil molecules that are often used as sensitizers in radiotherapy or in combination in chemotherapies. A good understanding of the primary processes involved in such simple systems should provide key information at the molecular level to feed more global models attempting to address the underlying causes of radio-sensitivity and radiation damage.

ACKNOWLEDGMENTS

The authors wish to thank to COST Action P9 network.

REFERENCES

1. B. Glimelius, U. Isacsson, E. Blomquist, E. Grusell, B. Jung and A. Montelius, *Acta Oncologica*, **38**, p. 137 (1999).
2. R.R. Wilson, *Radiology*, **47**, p. 487 (1946).
3. A. Brown and H. Suit, *Radiotherapy and Oncology,* **73**, p. 265–268 (2004).
4. T. Gohongi, K. Tokuuye, H. Iida, R. Nakai, N. Gunji, Y. Akine and K. Orii *Jpn J Clin Oncol*, 35, p. 40 (2005).
5. J. Cz. Dobrowolski, J. E. Rode, Robert Kołos, Michał H. Jamro´z, Krzysztof Bajdor, and Aleksander P. Mazurek, *J. Phys. Chem. A* **109**, p. 2167 (2005).
6. J. H. D. Eland, *Meas. Sci. Technol.* **4**, p. 1522 (1993).
7. B. Deconihout, P. Gerard, M. Bouet, and A. Bostel, *Appl. Surf. Sci.* **94**, p. 422 (1996).
8. P. Moretto-Capelle, A. Le Padellec, G. Brière, S. Massou, and F. Franceries, *J. Chem. Phys.* **127**, 234311 (2007).
9. P. Moretto-Capelle, D. Bordenave-Montesquieu, and A. Bordenave-Montesquieu, *J. Phys. B* **33**, p. L539 (2000).
10. J. H. D. Eland, *Mol. Phys.* **61**, p. 725 (1987).
11. P. Moretto-Capelle, A. Le Padellec, *Phys. Rev. A* **74,** 062705 (2006).
12. L. Sanche, *Eur. Phys. J. D.* **35**, p. 367 (2005).